

ASSESSING HORIZONTAL POSITIONAL ACCURACY OF GOOGLE EARTH IMAGERY IN THE CITY OF MONTREAL, CANADA

Mohammad Ali GOUDARZI, René Jr. LANDRY

*École de technologie supérieure (ÉTS), Laboratory of Space technologies, Embedded System, Navigation and Avionics (LASSENA), 1100 rue Notre Dame Ouest, Montreal (QC), H3C 1K3, Canada
E-mail: mohammad-ali.goudarzi.1@ens.etsmtl.ca (corresponding author)*

Received 06 February 2017; accepted 10 May 2017

Abstract. The horizontal positional accuracy of Google Earth is assessed in the city of Montreal, Canada, using the precise coordinates of ten GPS points spatially distributed all over the city. The results show that the positional accuracy varies in the study area between ~0.1 m in the south to ~2.7 m in the north. Furthermore, two methods are developed for correcting the observed positional errors: (a) using a set of transformation parameters between true coordinates of the geodetic points and their coordinates in Google Earth, and by (b) interpolating the misfit vectors at the geodetic points. The former method reduces the overall accuracy to ~67 cm RMSE, whereas the latter one practically removes all the distortion (RMSE = 1 cm). Both methods can be developed for other places in the world subject to availability of appropriate control points. In addition, a displacement problem caused by the topography of the area and the viewing angle of the imaging satellite is discussed, and it is shown that the true positions can be shifted even up to several meters, as a consequence.

Keywords: map calibration, Google Earth, GPS, navigation.

Introduction

Among the free and publicly available global image services such as Google Earth (2016), Google Maps (2016), NASA World Wind (2011), Microsoft Bing Maps (2016), and Apple Maps (2016), the first one is the most versatile and flexible service that is provided as a free and multiplatform standalone desktop software. The Google Earth (GE) software gives access to satellite and aerial images, ocean bathymetry, and other geospatial data such as roads and borders and their descriptive data as well as providing a range of tools such as flight simulator and street view. GE uses geographical coordinate system (latitude and longitude) on the World Geodetic System of 1984 (WGS 84) reference ellipsoid, which is the same datum used by Global Positioning System (GPS). Furthermore, it is available on all the major desktop and mobile operating systems in more than 40 languages.

GE also allows users to add their own spatial content such as satellite images, maps, photographs, landmarks, and descriptive information. This diversity in functionality along with the access to the underlying

images through its Application Program Interface (API), makes GE a unique platform for being used by or embedded in other systems, e.g., Web Map Service (WMS) servers/clients. GE has even found his path to elementary school classrooms and is now widely being used for teaching geography, history, and science (Richard 2014; Google Earth Community 2016).

Despite its numerous advantages, the positional accuracies of GE imagery are not officially published. Even though they are not expected to make damage in many projects or studies, lack of this information can potentially make problem in the tasks requiring a higher positional accuracy, such as autonomous navigation. This issue is an important challenge against using GE in precise and sensitive applications. Therefore, it is necessary to assess the positional accuracies of GE imagery before using them in such applications.

GE images are not orthorectified and do not have photogrammetric accuracy. They are collected from satellite images with world-wide coverage, aerial photos from local or national mapping agencies, and near-orthophoto collections in GeoPortals (Scollar 2013), and therefore, do not have an identical spatial

resolution or positional accuracy over the globe. Users may only know the name of the imaging satellite at certain levels of zoom. The source of the GE's elevation data is even more ambiguous. GE possibly uses the Digital Elevation Model (DEM) collected by Shuttle Radar Topography Mission (SRTM) from NASA (Mohammed *et al.* 2013), or the global DEM (GDEM) collected by the Advanced Spaceborne Thermal Emission and Reflection Radiometer (ASTER) instrument onboard the Terra satellite jointly provided by the Ministry of Economy, Trade, and Industry (METI) of Japan, and NASA. The SRTM DEM (Farr *et al.* 2007) was previously produced with the spatial resolution of 30 m and 90 m for the United States and other parts of the world, respectively. However, since United Nations Climate Summit in 2014, it is released with the higher resolution for everywhere (SRTM 2016). The ASTER GDEM (Tachikawa *et al.* 2011) with the spatial resolution of 30 m, however, has a better global coverage compared to the SRTM DEM. Some other sources mention that GE appears to use a range of DEM data sources to derive elevation data (Crosby 2010).

In the science of mapping, position of a real world entity is defined by some numbers in an appropriate coordinate system. Then, positional accuracy is defined as the closeness of those numbers to the true position of the entity in that system (Guptill, Morrison 1995: 32), and is traditionally divided to: (a) horizontal, and (b) vertical positional accuracies. There are other measures of accuracy such as temporal accuracy, attribute accuracy, logical consistency, and completeness (Kemp 2008: 2); however, this study focuses on the evaluation of the horizontal positional accuracy of GE over the city of Montreal, Canada. The vertical positional accuracy of GE is not addressed because it has already been studied by other researchers (e.g., Berry *et al.* 2007). The advantage of this study compared to other similar studies is that, along with evaluating the horizontal positional accuracy, it provides two methods for correcting GE images that makes them suitable for applications with higher precision, and discusses the effect of the relief displacement issue as well.

This paper has the following structure. Section 1 briefly reviews other similar studies in order to give an overview of the positional accuracy of GE images in different parts of the world. Then Section 2 introduces the study area and the data set. The reason for choosing this area and the criteria for selecting the data set are addressed in this section. In Section 3, the research methodology is presented along with the results and analysis. Then, two methods for correcting GE images

are developed and compared in Sections 3.1 and 3.2, respectively. The comparison is based on the numerical results obtained for the study area. Section 4 discusses the methods and results, and Section 5 presents the validation of the second method as a superior approach using another set of GPS observations for a long trajectory around the city of Montreal. In this section, other reasons for the inaccuracies in GE maps are presented. Finally, the findings of this research will be summarized and concluded in the last section.

1. Background

Since its public release in 2005 (Moore 2007), GE has found a wide range of non-profit applications from personal exploration to rescue victims of natural disasters. A long range of case studies can be found in the Google Earth Outreach website (2016). Scientific community also has used GE imagery in several technical and scientific applications, such as studying land use and land cover, agriculture, earth surface process and geomorphology, landscape, habitat availability, biology, health, and surveillance systems. According to Yu and Gong (2012), the use of GE in research projects can be summarized in eight categories of: visualization, data collection, validation, data integration, communication and dissemination, modelling, data exploration, and decision support. A comprehensive list of applications of GE in scientific projects can be found in Pulighe *et al.* (2015). Its popularity in scientific community as well as its high-resolution image database, which is often updated, deludes users to assume GE imagery is a credible and accurate source of spatial and geographical data or information. This illusion is even more fortified by the number of decimal places of the coordinates shown at the bottom of GE application window at any zoom level. Currently, latitude and longitude coordinates are shown by six decimal places that are equal to a precision of ~10 cm, which is obviously not true.

Many researchers have studied the positional accuracy of GE imagery using different methods. Potere (2008) compared GE high resolution images with Landsat GeoCover scenes over a global sample of 436 control points located in 109 cities worldwide. According to that, GE control points showed a positional accuracy of 39.7 m RMSE. This reduces to 24.1 m RMSE for more developed countries. Another study by Becek and Ibrahim (2011) has shown a wide range of positional accuracy from 10 m to more than 1.5 km for 2045 runways inspected in five continents.

Scollar (2013) classified errors in the GE images into three groups of horizontal and vertical displacements, height, and tilt effect (orthorectification), and distortion due to bad matching of multiple images. A mislocation between 5 to 10 m was reported in this study for the center of images that is mainly attributed to manual image matching. In another study, Ubukawa (2013) compared the horizontal positional accuracy of five geospatial data sets including GE with the ALOS/PRISM imagery for 10 cities in different regions of the world. In this study, the author determined a RMSE value of 8.2 m in GE images. Mohammed *et al.* (2013) estimated the GE horizontal and vertical accuracies in Khartoum State, Sudan, by comparing coordinates of 16 points measured in GE and measured by a Trimble 5800 GPS receiver in the Real Time Kinematic (RTK) mode. They computed RMSE of 1.8 m and 1.7 m for horizontal and vertical coordinates, respectively. They mentioned that while the altimetric accuracy of GE is constant during time, its planimetric accuracy is improving. Farah and Algarni (2014) assessed the positional accuracy of GE in Riyadh, Saudi Arabia, by comparing coordinates of nine GPS points located in a small area and their coordinates in GE. The result showed horizontal accuracy of 2.2 m RMSE. Ragheb and Ragab (2015) studied horizontal positional accuracy of GE for a small area in Cairo, Egypt, using 16 surveying control points, and obtained the accuracy of 10.6 m RMSE before georeferencing the GE image. These examples, among others, firstly indicate the positional accuracy of GE imagery is improving, and secondly confirm that GE uses different image data sets for different parts of the world.

2. Study area and data

The study area is the city of Montreal located in the southwest of the province of Quebec (Fig. 1). It is the

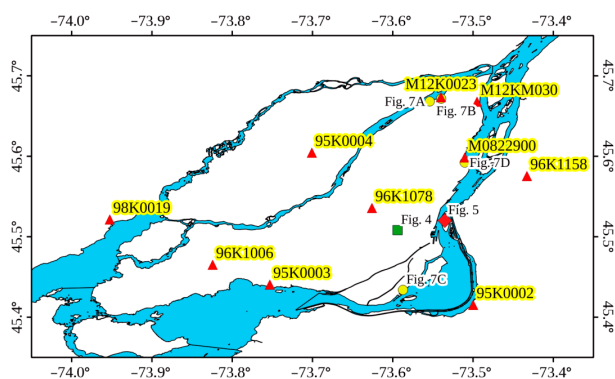


Fig. 1. Spatial distribution of the selected GPS points (red triangles) over the city of Montreal and the suburbs. The figure also shows locations of Figs 4, 5, and 7

second major city in Canada covering more than 4258 km² (StatCan 2016a) including metropolitan area with the estimated population of more than 4 million inhabitants for 2015 (StatCan 2016b). In general, the city has a flat or a slightly hilly topography, except for a three-peak hill called Mount Royal with the elevation of 232 m above the sea level for the highest peak. This city was selected for evaluating the horizontal positional accuracy of GE imagery according to field tests required in the Vehicle Tracking and Accident Diagnostic System (VTADS) project. VTADS is a research project under development at Laboratory of Space technologies, Embedded System, Navigation, and Avionics (LASSENA) of École de Technologie Supérieure (ÉTS), Montreal, Canada. One of the aims of the project is to establish new design methods and advanced sensor fusion techniques for robust and efficient automotive navigation and optimal fleet management in harsh environments with a horizontal positional accuracy of better than one meter. Therefore, findings of this research make an important contribution to use corrected globally georeferenced satellite images for performing the location based field tests of the project.

For the accuracy assessment, ten proper GPS points were selected across the city of Montreal from the geodetic network installed and measured by Ministry of Energy and Natural Resources of Quebec (MERNQ 2014) with geodetic-grade GPS receivers. The network comprises more than 1900 GPS points with 18 permanent GPS reference stations that covers southern part of the province of Quebec. MERNQ provides precise coordinates of the GPS points in the form of standard description pages available at Géoboutique Québec (2013) along with their descriptive information. Although the selected points have permanent and stable monuments and are clearly visible in GE images with a good color contrast, they were all investigated by performing a field work to avoid any misunderstanding of nearby similar entities in GE images. Figure 1 displays the location of the selected GPS points and their codes in the Géoboutique system, as well as locations of some other test points shown in Figures 4, 5, and 7.

Starting from version 5, it is possible to browse the archive of GE and assess the temporal accuracy of images. In this research, however, the horizontal positional accuracy of images dated on September 17, 2013 was assessed. Although this is not the most recent image in the archive, it is the one that is loaded by default in both GE and Google Maps (GM) and covers all the study area seamlessly.

3. Methods and results

The horizontal positional accuracy of GE was analyzed by comparing the two dimensional coordinates of the selected GPS points with their coordinates measured in GE. Coordinates of the GPS points in GE were measured by hovering the mouse cursor on the most probable location of the GPS markers and with respect to the observations in the field work. The measurements were repeated several times to avoid any mislocation and misinterpretation of the GPS points. The measured and the reference coordinates of the points are shown in Table 1. In this table, misfit vectors are defined as the directional distances from GE coordinates to GPS coordinates and were calculated using the *distance* function of MATLAB on the WGS84 ellipsoid. As the table shows, misfit vectors have wide ranges in both length and heading angle: while the minimum length of 0.13 m is observed at point 95K0003 in the south, the maximum length reaches 2.71 m at point M12K0023 in the north.

The misfit vectors are graphically represented in Figure 2. In general, they are smaller in the south of the city, while they are larger at the northeast. A horizontal root mean squared error (RMSE) of 1.08 m was calculated according to the formula recommended by the Federal Geographic Data Committee of the United States (FGDC 1998: 10):

$$RMSE = \sqrt{\frac{\sum_{i=1}^{n_p} \left((n_{GPS,i} - n_{GE,i})^2 + (e_{GPS,i} - e_{GE,i})^2 \right)}{n_p}}, \quad (1)$$

where n and e are the north and east coordinates of the i th GPS and GE points with proper subscripts after

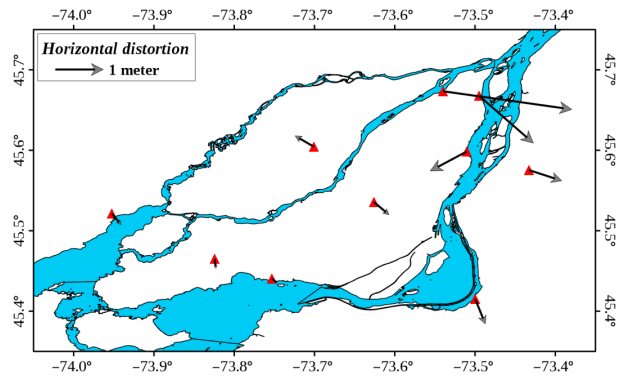


Fig. 2. Misfit vectors between true GPS and GE coordinates calculated for the GPS points

transferring the geographical coordinates in Table 1 to the Universal Transverse Mercator (UTM) projection system, and n_p is the number of points.

3.1. Similarity transformation

In order to make GE images useful in applications that require higher positional accuracy, a two-dimensional similarity transformation (Kraus 2007: 14) between GPS and GE coordinates was developed as:

$$\mathbf{X}_{GE} = \Delta\mathbf{X} + \mu\mathbf{R}\mathbf{X}_{GPS}, \quad (2)$$

where \mathbf{X} shows GE and GPS coordinates vector (two parameters of n and e) with respect to the subscripts, $\Delta\mathbf{X}$ is the translation vector (two parameters of Δn and Δe), \mathbf{R} is the rotation matrix (one parameter of α), and μ is the scale factor (one or two parameters). Equation (2) is written in a way that GPS coordinates are transformed to the GE coordinates, while the other way is ideally desired. This choice is reasonable because: (a) the objective of the transformation is to match GPS coordinates over GE images and use them as a base map, and (b) if not

Table 1. True GPS and GE coordinates and their differences (misfit vectors) for the selected GPS points

No	Point code	GPS coordinates		GE coordinates		Misfit vectors	
		Latitude (°)	Longitude (°)	Latitude (°)	Longitude (°)	Length (m)	Heading (°)
1	95K0002	45.4153587	-73.4998767	45.4153540	-73.4998740	0.56	158
2	95K0003	45.4405837	-73.7531573	45.4405830	-73.7531560	0.13	127
3	96K1006	45.4652048	-73.8243883	45.4652030	-73.8243880	0.20	173
4	98K0019	45.5214781	-73.9525385	45.5214760	-73.9525360	0.30	140
5	95K0004	45.6044980	-73.7008240	45.6045000	-73.7008290	0.45	300
6	M12K0023	45.6734382	-73.5400025	45.6734350	-73.5399680	2.71	98
7	M12KM030	45.6678419	-73.4950785	45.6678330	-73.4950640	1.50	131
8	M0822900	45.5985626	-73.5103672	45.5985590	-73.5103770	0.86	242
9	96K1158	45.5754880	-73.4329218	45.5754860	-73.4329130	0.72	108
10	96K1078	45.5357554	-73.6259920	45.5357530	-73.6259880	0.41	130

impossible, it is very difficult from programming point of view to transform the GE images. Depending on the number of parameters for the scale factor (2), can be expanded to a 4-parameter model, as:

$$\begin{bmatrix} n_i \\ e_i \end{bmatrix}_{GE} = \begin{bmatrix} 1 & 0 & e_i & n_i \\ 0 & 1 & -n_i & e_i \end{bmatrix}_{GPS} \begin{bmatrix} \Delta n \\ \Delta e \\ \alpha \\ \mu \end{bmatrix} \quad (3)$$

or a 5-parameter model, as:

$$\begin{bmatrix} n_i \\ e_i \end{bmatrix}_{GE} = \begin{bmatrix} 1 & 0 & e_i & n_i & 0 \\ 0 & 1 & -n_i & 0 & e_i \end{bmatrix}_{GPS} \begin{bmatrix} \Delta n \\ \Delta e \\ \alpha \\ \mu_n \\ \mu_e \end{bmatrix} \quad (4)$$

Equations (3) and (4) were solved for 4 or 5 unknown parameters, respectively, with an over-determined least-squares method using the points listed Table 1. True GPS and GE coordinates and their differences (misfit vectors) for the selected GPS points. 1 after transferring them to the UTM projection system. The degree of freedom is 16 and 15 for the former and latter model, respectively. The results are shown in Table 2. The table shows that scale factors are practically the same in latitudinal and longitudinal directions, and the rotation angle is close to zero. Therefore, the

translation is the main effective factor for correcting the GE images in this area. Both models reduce the RMSE to 0.67 m, which is a good overall improvement especially for northern parts of the study region where misfit error of greater than 2 m are observed.

3.2. Interpolating misfit vectors

This method is based on direct interpolation of misfit vectors. For the interpolation, it is assumed that there is no spatial correlation between east and north components of the misfit vectors. Therefore, the algorithm consists in the interpolation of each component of the misfit vectors separately using the universal kriging method with a variogram analysis (Gebbers 2015, sec. 7.11). The outcome would be two raster layers of correcting values in north and east directions. Since this method of interpolation is independent of the grid size, the pixels of the raster layers can be selected at any arbitrary size.

Figure 3 shows the result of interpolation on a grid of 0.02°×0.02° resolution. The area out of the convex hull formed by the GPS points was discarded. This consideration avoids extrapolation of the data that principally has less accuracy or higher standard deviation. As the figure shows, the interpolated misfit vectors are larger in the north and smaller in the south. In this method, the RMSE value reduces to 0.01 m, which is practically negligible.

Table 2. Parameters of the similarity transformation

Unknown parameters		4-parameter solution	5-parameter solution
Translation	Δn (m)	-0.296721	-0.296721
	Δe (m)	0.424755	0.424755
Rotation	α (°)	-0.001369	-0.001250
Scale factor	μ_n	1.000011	1.000004
	μ_e		1.000014

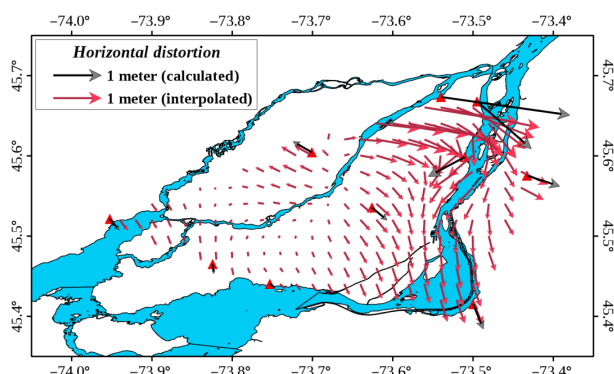


Fig. 3. Representation of interpolated misfit vectors showing a continuous deformation and a very well fit to local variations

4. Discussion

As mentioned in Section 1, positional accuracy of GE images is not the same all over the globe. It is even different over one city that might be resulted from stitching different image sources. In the case of Montreal, the magnitude of the misfit vector varies from about 10 cm in the south to about 2.7 m in the northeast. Misfit vectors have different directions that indicate a horizontal distortion in the GE images across the city. The RMSE value obtained in this research is considerably smaller than those reported in other studies. This is partly because this analysis was done using geodetic quality reference points with very small altitude with respect to the nearby terrain for the comparison. Accuracy of these points is few centimeters that are practically negligible with respect to the horizontal positional accuracy of GE images. The other reason can be a better quality of GE images for metropolitan areas, which are also updated more frequently.

Two new methods were developed in this study for adapting GE images for navigation purposes,

namely: similarity transformation, and direct interpolation of misfit vectors. Since transforming GE images is very difficult in practice, it was decided to transform the observed GPS points in the opposite direction but with the same magnitude according to the horizontal positional error of GE images at the observation point. The advantage of the similarity transformation is that it is simple and can transform a large number of GPS points efficiently. However, it decreases the horizontal positional accuracy for southern part of the study area where the magnitudes of the misfit vectors are in the range of 13 cm to 20 cm (i.e., smaller than the RMSE value). The second problem of this method is that, the transformation parameters are mainly affected by the large misfit vectors in the north and therefore tends to shift all the points toward southeast. However, Figure 2 shows that not all the misfit vectors have the same direction. At points 95K0004 and M0822900, for example, misfit vectors are pointing toward northwest and southwest, respectively, and do not follow the general trend of the transformation. Therefore, the direction of the correction might be incorrect in some parts like these two points.

Misfit vectors were interpolated to overcome the limitations of the previous method. In the former method, the estimated parameters are mainly affected by magnitudes and directions of the misfit vectors included in the least-squares adjustment but not by their locations. In other words, if the location of a GPS point is changed arbitrarily while keeping the same misfit vector, the estimated parameters will not change considerably, but instead this mainly impacts the RMSE value. For example, the position of M12K0023 (the point with the largest misfit vector) was shifted toward southwest by 0.23° near 95K0003 (the point with the smallest misfit vector), and the 5-parameter model was recalculated. This resulted in less than 1 mm change in the translation, about 0.001° change in the rotation angle, and no change up to four decimal places in the scale factor. However, the RMSE value was reduced to 0.53 m. In the latter method, the interpolated vectors can follow the local variations of the misfit vectors in magnitude and direction that results in a very smaller RMSE value. According to theory of the kriging interpolation (Gebbers 2015: 295), this method is also sensitive to the location of GPS points used for the interpolation. As a result, the former method is more proper for the places with small spatial extend in which misfit vectors have generally the similar magnitudes and directions. However, this is not the case for the latter method and it can be used for large areas if

it is accompanied by variogram analysis to take into account the spatial correlation of control GPS points. Therefore, the method of direct interpolation of misfit vectors is more accurate than the method of similarity transformation; however it is computationally expensive, and is proper for server-based or post-processed applications.

Although both models can improve inaccuracies in horizontal positioning of images, they cannot account for horizontal displacements caused by topography of the area or tilt of the imaging camera. The former issue, called relief displacement, is defined as a shift in the image position of an object that is caused by its elevation above or below a particular datum. In vertical or near vertical images, the shift is radial from the nadir point. The magnitude of the relief displacement is directly proportional to elevation of the object with respect to the datum surface, and radial distance between the object and the nadir point, and inversely proportional to the altitude of the imaging camera above the datum (Pandey 1987: 50). A sample of distortion caused by the relief displacement is shown in Figure 4a for Mount Royal, the city of Montreal. As the figure shows, the roads are not matched with their footprint in the satellite image on top of the hill, and are shifted with respect to altitude of the topography and the geometry of the imaging satellite. This can be corrected in GM by correcting the elevation effect using a DEM, as shown in Figure 4b. However, this option is not available in GE.

The relief displacement was further investigated by performing a field test in which a trajectory was measured over high bridges and roads using the same equipment and setup for the validation (Section 5). Figure 5a clearly shows this effect in east–west direction over the central part of the Jacques Cartier Bridge, located in the Saint Helen’s Island, near Montreal. This



Fig. 4. Relief displacement in Mount Royal, the city of Montreal, (A) before, and (B) after correction. This location is marked by a green square in Fig. 1

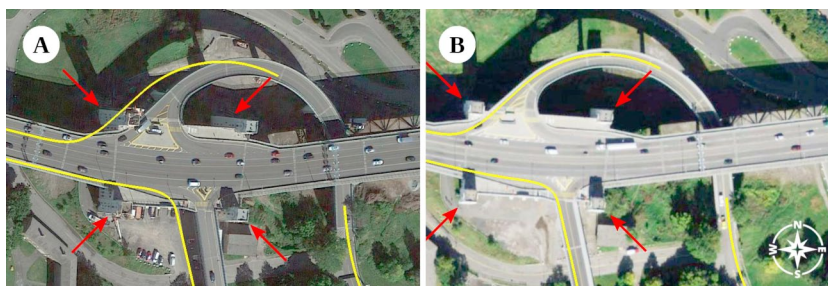


Fig. 5. (A) Relief displacement over the central part of the Jacques Cartier Bridge, the city of Montreal. (B) The displacement is reduced when the relief is near the nadir point. The yellow line shows the trajectory measured with the GPS receiver, and red arrows point to the four towers around the structure.

This location is marked by a red diamond in Fig. 1

part of the bridge has been constructed on top of a three-story building surrounded by four towers at each corner (shown by red arrows), and has an approximate height of more than 43 m above the water level. In reality, the towers are vertical and their facets should not be visible from a perpendicular top view. However, they are visible especially for those located in the western side due to a big off-nadir viewing angle. This shift amounts to more than 12 m that is close to the distance between the GPS trajectory (shown by yellow line) and the center line of the road. This indicates that if the off-nadir angle is reduced, the image footprint will coincide to the trajectory. Figure 5b shows such an image acquired on September 22, 2008 for the same area found in the GE archive. The facets of the towers are very small in the second image, thus off-nadir angle and relief displacement are less in this part. As a result, the road is matched with the trajectory. This type of relief displacement can theoretically be corrected like in the previous example if a digital surface model (DSM) is available. However, because DSM is not generally available in GE or GM, the relief displacement remains uncorrected in both systems.

5. Validation of the method of interpolating misfit vectors

As discussed in the previous section, the method of interpolating misfit vectors is superior to the similarity transformation method in terms of accuracy. To test the strength of this method, a field work was performed for validating the results obtained in Section 3.2. First, a trajectory was designed around the city of Montreal within the convex hull formed by the GPS points and near open waterbodies, as much as possible. The reasons are: (a) to have more precise correction values by staying inside of the GPS convex hull, and (b) to avoid the relief displacement by remaining on low altitude areas, respectively. In designing the trajectory, an important consideration was given to the trend in the magnitude of the misfit vectors, which is in southwest–northeast direction, to investigate the effect of the correction on the lowest and highest magnitude misfit vectors. The designed trajectory is shown in Figure 6 with a thick red line. In this figure, contour lines and its background raster show the magnitude of the correction in meter calculated from the two raster layers of correcting values in north (Δn) and east (Δe) directions obtained in Section 3.2 as $\sqrt{\Delta n^2 + \Delta e^2}$.

The trajectory was surveyed with a geodetic grade Novatel ProPak6 GNSS receiver with a zephyr antenna installed on the roof of the laboratory's vehicle in the kinematic mode. This setup provides the maximum possible sky visibility especially in urban areas. The data were processed using precise point positioning (PPP) method with the Novatel Inertial Explorer software. Then, the corresponding correction vectors were extracted from the interpolated misfit vectors and were applied to processed points using QGIS software (QGIS Development Team 2015).

The uncorrected GPS points (purple dots) and the corrected trajectory (red line) in northeast (A and

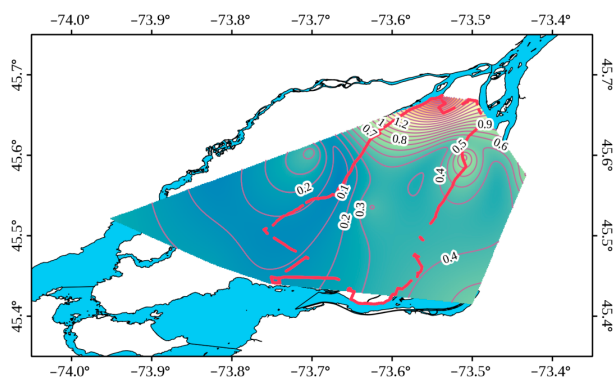


Fig. 6. The test trajectory for validating the results. Contour lines show the magnitude of correction in meter

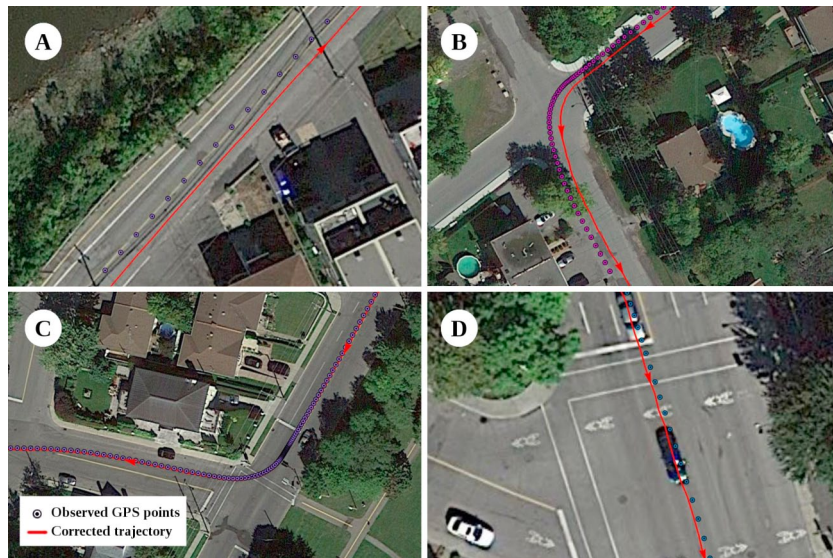


Fig. 7. Snapshots of the uncorrected GPS points (purple dots) and the corrected trajectory (red line) for (A and B) northeast, (C) southeast, and (D) east of the study area, where the correction is higher. Arrows on the trajectory show the direction of the driving. These locations are marked by yellow circles in Fig. 1

B), southeast (C), and east (D) of the study area are compared in Figure 7. The figure shows that the uncorrected trajectory is shifted toward center line of the road or sidewalk, whereas the corrected trajectory locates in the middle of the lane where it has the most probability of driving. While in northeast and east the magnitude of the correction is meaningful, it is small or practically negligible in southeast.

Conclusions

The horizontal positional accuracy of Google Earth (GE) imagery was studied over the city of Montreal using precise position of ten GPS points. The magnitude of the misfit vectors ranges between 0.13 m in the south and 2.7 m in the northeast of the city with the RMSE value of 1.08 m, which shows a general trend in southwest–northeast direction. In terms of direction, misfit vectors are mostly pointing toward southeast, however, some counterexamples are observed. The lower RMSE value in this research compared to other studies shows that horizontal positional accuracy of GE imagery for the city of Montreal is better than those places. However, this amount is yet important for precise applications and shows a spatial variation over the study area. This hints that for such applications, the reliability of the GE images should first be inspected by a field work operation, and then be corrected if they do not meet the required positional accuracy.

This paper further provided two new and practical methods for enhancing the horizontal positional

accuracy using (a) similarity transformation and (b) direct interpolation of the misfit vectors, when inaccuracies are due to georeferencing images (Kraus 2007: 404). The former method is simpler and computationally more efficient. It could reduce the overall RMSE for misfit vectors to 0.67 m over the study area. However, it has the disadvantage of decreasing or distorting accuracy in areas that have a better accuracy than the overall RMSE value, or where misfit vectors have different direction with the overall bias. The latter method can practically correct the entire misfit, but it is computationally expensive and is more suitable for server based applications. Neither of models can account for horizontal inaccuracies when they are caused by relief displacement (non-orthorectified images). In this case, they might be corrected using a DEM or DSM of the area or structures. The concept developed in this research are generic and similar models can be adapted for any other part of the world subject to availability of such accurate and permanent geodetic points with clear visibility in GE images.

Acknowledgements

This project has been funded by Natural Sciences and Engineering Research Council of Canada (NSERC) and PROMPT under a Collaborative Research and Development (CRD) project with iMetrik and Future Electronics companies. In addition, QGIS, GIMP, and Inkscape software were used for preparing figures of this paper.

References

- Apple Maps. 2016. *iOS 9- Maps- Apple* [online]. Apple Inc. [cited 13 June 2016]. Available from Internet: <https://www.apple.com/ios/maps/>
- Becek, K.; Ibrahim, K. 2011. On the positional accuracy of the Google Earth™ imagery, in *FIG Working Week 2011 Bridging the Gap between Cultures*, 18–22 May 2011, Marrakech, Morocco.
- Berry, P. A. M.; Garlick, J. D.; Smith, R. G. 2007. Near-global validation of the SRTM DEM using satellite radar altimetry, *Remote Sensing of Environment* 106: 17–27.
- Bing Maps. 2016. *Bing Maps – directions, trip planning, traffic cameras and more* [online]. Bing Maps [cited 13 June 2016]. Available from Internet: <http://www.bing.com/mapspreview>
- Crosby, C. 2010. LiDAR Beginning to Appear in Google Maps Terrain Layer [online]. OpenTopography [cited 14 July 2016]. Available from Internet: <http://www.opentopography.org/blog/lidar-beginning-appear-google-maps-terrain-layer>
- Farah, A.; Algarni, D. 2014. Positional accuracy assessment of GoogleEarth in Riyadh, *Artificial Satellites* 49: 101–106. <https://doi.org/10.2478/arsa-2014-0008>
- Farr, T. G.; Rosen, P. A.; Caro, E.; Crippen, R.; Duren, R.; Hensley, S.; Kobrick, M.; Paller, M.; Rodriguez, E.; Roth, L.; Seal, D.; Shaffer, S.; Shimada, J.; Umland, J.; Werner, M.; Oskin, M.; Burbank, D.; Alsdorf, D. 2007. The shuttle radar topography mission, *Reviews of Geophysics* 45, RG2004. <https://doi.org/10.1029/2005RG000183>
- FGDC. 1998. *Geospatial Positioning Accuracy Standards. Part 3: National Standard for Spatial Data Accuracy (No. FGDC-STD-007.3-1998)*. Federal Geographic Data Committee. Reston, VA, the USA.
- Gebbers, R. 2015. Geostatistics and Kriging, in M. Trauth. *MATLAB Recipes for Earth Sciences*. Berlin, Heidelberg: Springer Berlin Heidelberg, 427.
- Géoboutique Québec. 2013. *Géoboutique Québec* [online]. Gouv. du Québec [cited 21 June 2016]. Available from Internet: <http://geoboutique.mern.gouv.qc.ca/edel/pages/recherche/critereRechercheEdel.faces>
- Google Earth Community. 2016. *Google Maps Education* [online]. Google Inc. [cited 5 July 2016]. Available from Internet: <https://www.google.com/help/maps/education/>
- Google Earth outreach. 2016. *Google Earth outreach* [online]. Google Inc. [cited 21 June 2016]. Available from Internet: <http://www.google.com/earth/outreach/index.html>
- Google Earth. 2016. *Google Earth* [online]. Google Co. [cited 13 June 2016]. Available from Internet: <https://www.google.com/earth/>
- GoogleMaps. 2016. *Google Maps* [online]. Google Co. [cited 13 June 2016]. Available from Internet: <https://www.google.ca/maps/>
- Guptill, S. C.; Morrison, J. L. (Eds.). 1995. *Elements of spatial data quality*. Pergamon Press.
- Kemp, K. K. (Ed.). 2008. *Encyclopedia of geographic information science*. SAGE Publications.
- Kraus, K. 2007. *Photogrammetry*. De Gruyter textbook. 2nd ed. Berlin, New York: Walter De Gruyter. <https://doi.org/10.1515/9783110892871>
- MERNQ. 2014. *Geodetics and GPS technology* [online]. Minister of Energy and Natural Resources Quebec [cited 17 December 2014]. Available from Internet: <http://www.mern.gouv.qc.ca/english/territory/expertise/expertise-geodetics.jsp>
- Mohammed, N. Z.; Ghazi, A.; Mustafa, H. E. 2013. Positional accuracy testing of Google Earth, *International Journal of Multidisciplinary Sciences and Engineering* 4: 6–9.
- Moore, R. 2007. *Introducing Google Earth Outreach* [online]. Google Inc. [cited 21 June 2016]. Available from Internet: <https://googleblog.blogspot.ca/2007/06/introducing-google-earth-outreach.html>
- Pandey, S. N. 1987. *Principles and applications of photogeology*. New Age International Publisher.
- Potere, D. 2008. Horizontal positional accuracy of Google Earth's high-resolution imagery archive. *Sensors* 8: 7973–7981. <https://doi.org/10.3390/s8127973>
- Pulighe, G.; Baiocchi, V.; Lupia, F. 2015. Horizontal accuracy assessment of very high resolution Google Earth images in the city of Rome, Italy, *International Journal of Digital Earth* 9(4): 342–362. <https://doi.org/10.1080/17538947.2015.1031716>
- QGIS Development Team. 2015. *QGIS Geographic Information System*.
- Ragheb, A. E.; Ragab, A. F. 2015. Enhancement of Google Earth positional accuracy, *International Journal of Engineering Research & Technology* 4(1): 627–630.
- Richard, G. A. 2014. *Teaching with Google Earth* [online]. Pedagogy in Action [cited 4 July 2016]. Available from Internet: http://serc.carleton.edu/sp/library/google_earth/index.html
- Scollar, I. 2013. Google Earth: improving mapping accuracy, *AARGnews* 47: 19–27.
- SRTM. 2016. *Shuttle Radar Topography Mission* [online]. Jet Propulsion Laboratory, California Institute of Technology [cited 14 July 2016]. Available from Internet: <http://www2.jpl.nasa.gov/srtm/>
- StatCan. 2016a. *Montréal metropolitan area census profile* [online]. Statistica Canada [cited 7 July 2016]. Available from Internet: <http://www12.statcan.gc.ca/census-recensement/2011/dp-pd/prof/details/page.cfm?Lang=E&Geo1=CMA&Code1=462&Geo2=PR&Code2=01&Data=Count&SearchType=Begins&SearchPR=01&B1=All>
- StatCan. 2016b. *Population of census metropolitan areas* [online]. Statistica Canada [cited 7 July 2016]. Available from Internet: <http://www.statcan.gc.ca/tables-tableaux/sum-som/l01/cst01/demo05a-eng.htm>
- Tachikawa, T.; Hato, M.; Kaku, M.; Iwasaki, A. 2011. Characteristics of ASTER GDEM version 2, in *IEEE International Geoscience and Remote Sensing Symposium (IGARSS)*, 24–29 July 2011, Vancouver, Canada. IEEE, 3657–3660. <https://doi.org/10.1109/igarss.2011.6050017>
- Ubukawa, T. 2013. *An evaluation of the horizontal positional accuracy of Google and Bing Satellite Imagery and Three roads data sets based on high resolution satellite imagery*. Center for Earth Science Information Network.
- NASA World Wind. 2011. *NASA World Wind* [online]. Natl. Aeronaut. Sp. Adm. [cited 8 July 2016]. Available from Internet: <http://worldwind.arc.nasa.gov/java/>
- Yu, L.; Gong, P. 2012. Google Earth as a virtual globe tool for Earth science applications at the global scale: progress and perspectives, *International Journal of Remote Sensing* 33(12): 3966–3986. <https://doi.org/10.1080/01431161.2011.636081>

Mohammad Ali GOUDARZI. Dr holds a PhD degree in Geodesy from Laval University, Canada. He has been post-doctorate researcher at Laboratory of Space technologies, Embedded System, Navigation, and Avionics (LASSENA) at École de Technologie Supérieure (ÉTS), Montreal, for one year. During this period, he participated in the Vehicle Tracking and Accident Diagnostic System (VTADS) and worked on advanced sensor fusion techniques for autonomous navigation and optimal fleet management in harsh environments. He is currently works at Canadian Geodetic Survey as a geodetic engineer on real-time GNSS orbit improvement.

René Jr. LANDRY. Dr received an electrical engineering degree at École Polytechnique of Montreal in 1992, a Master of Science in Satellite Communication engineering in 1993, a DEA in microwave in 1994 and a PhD in GNSS anti-jamming at SupAero in 1998. Since 1999, he is professor at the department of electrical engineering at École de Technologie Supérieure (ÉTS), and the director of LASSENA laboratory. His expertise in embedded systems, navigation, and avionic is applied notably in the field of transport, aeronautic, and space technologies.